ELSEVIER

0144-8617(94)00052-2

Carbohydrate Polymers **25** (1994) 197–202

0144-8617/94/$07.00

Static light scattering technique applied to pectin in dilute solution. Part III: The tendency for association

Gisela Berth,[a*†] Herbert Dautzenberg[b] & Jürgen Hartmann[b]

[a]*Deutsches Institut für Ernährungsforschung Potsdam-Rehbrücke, Arthur-Scheunert-Allee 114–116, D-14558 Bergholz-Rehbrücke, Germany*
[b]*Max-Planck-Institut für Kolloid- und Grenzflächenforschung, Kantstr. 55, D-14513 Teltow-Seehof, Germany*

(Received 22 June 1993; accepted 7 February 1994)

The tendency for association was studied by light scattering applied to a series of a high-methoxyl citrus pectin solution in phosphate buffer. To prevent artefacts, the clarified stock solution and buffer were mixed within the measuring cell. The measured data are presented as Zimm and master plots. A reversible increase of the apparent molecular weight with rising polymer concentration and slightly negative second virial coefficients were found in the case of the uncentrifuged, but filtered, solutions, indicating a slight tendency for association. The associates formed remain relatively small. This is independent of the pore size of the filters used for clarification. Prepurification by ultracentrifugation gave solutions which showed two-component behaviour and gave no hint of association.

INTRODUCTION

Pectins are often said to have a strong tendency for association/aggregation since light scattering measures frequently give negative second virial coefficients (see Part I of this series). Their ability to form excellent gels even at concentrations below 1% (w/w) has been used to support this argument. This, however, is not conclusive as, apart from the undesired and non-reversible pregelation due to calcium ions, high-methoxyl pectins need considerable amounts of sugar (pectin plus sugar must reach 65% dry matter) and pH values below 3·2–3·4 for gelation. Low-methoxyl pectins require the addition of calcium ions to form three-dimensional networks via intermolecular bridges.

In our previous papers (Part I and II of this series) we have shown that conventional purification or clarification procedures including gel-permeation chromatography (GPC) are a mixed blessing. We could not achieve absolutely particle-free solutions, and the negative virial coefficients described in Part I could easily be a consequence of the heterogeneity of the matter itself. (It might have been similar problems which induced Smith & Stainsby (1977) to enzymically degrade their galacturonans after measurement in order to obtain the scattering intensities of the blank which was to be subtracted.) However, any kind of association could not be absolutely excluded because the way we had performed our experiments did not allow conclusions like this to be drawn. For that reason we have modified our experimental procedure.

To prevent artefacts due to filtration after the individual concentration steps, we prepared the clarified (dust-free) stock solution and buffer and mixed them within the measuring cell. We then measured the scattering intensities as a concentration and dilution series, respectively, by adding aliquots of the pectin solution to the buffer and vice versa. This was done for stock solutions 'clarified' by membrane filtration alone, or in combination with ultracentrifugation.

Data obtained are presented as Zimm plots (Zimm, 1948) and master plots (Dautzenberg & Rother, 1988, 1992).

EXPERIMENTAL

The pectin sample used is a commercial high-methoxyl citrus pectin (Koch-Light, UK) having both degrees of

*To whom correspondence should be addressed.
†Present address: Institute of Biotechnology, University of Trondheim, N-7034 Trondheim, Norway.

esterification and galacturonan contents of about 70%. It was dissolved in 0·037 M phosphate buffer of pH 6·5, containing 1 mmol l^{-1} Na_2 EDTA, by shaking overnight.

All light scattering measurements were performed by means of a 'Sofica' goniometer (Fica, France) equipped with a helium/neon laser light source of $\lambda = 632{\cdot}8$ nm (Zeiss Jena, Germany, or Uniphase, Germany).

The equidistant concentration series in Figs 1–3 were prepared by adding slowly and under stirring the dust-free prepurified stock solution to the buffer in the measuring cell by means of a medical infusion pump. After a short 'settling' time the light scattering intensities were measured at 31 angles between 30 and 150°. The concentration factor was checked by weight.

The other data on ultracentrifuged solutions were obtained after adding a fixed volume of the pectin solution to the buffer and vice versa (weight control). Buffers were treated correspondingly.

The software package used on an AC 7100 personal computer (Robotron, Germany) was written by Dr

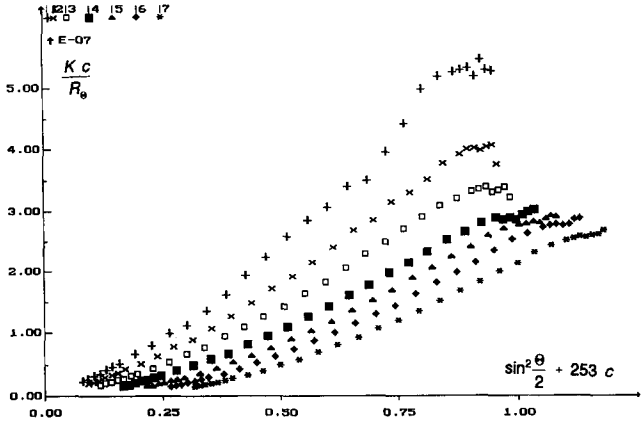

(a)

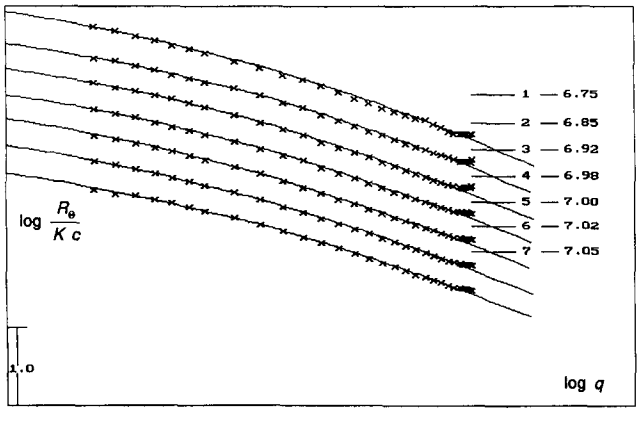

(b)

Fig. 1. (a) Zimm and (b) master plot obtained on a concentration series after filtration through a 5·0 μm pore size filter (see Table 1).

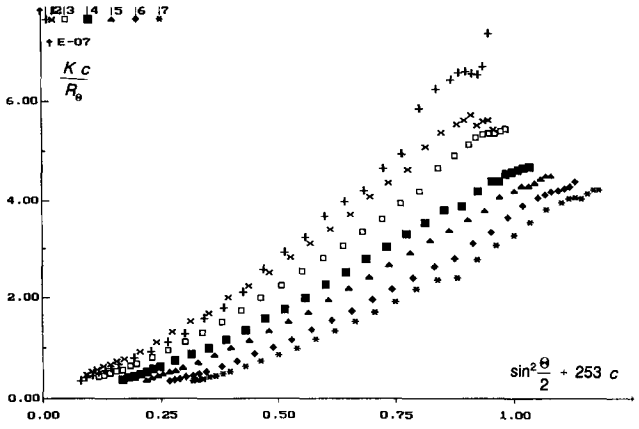

(a)

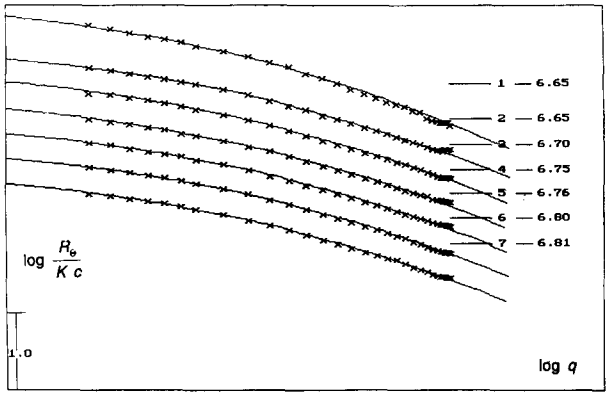

(b)

Fig. 2. (a) Zimm and (b) master plot obtained on a concentration series after filtration through 5·0/1·2 μm pore size filters (see Table 1).

Gudrun Rother (Max-Planck-Institut für Kolloid- und Grenzflächenforschung, Teltow-Seehof).

RESULTS AND DISCUSSION

Figures 1–3 present a collection of Zimm and master plots obtained when aliquots of the purified stock solution were added to the clean buffer. The lowest and the highest concentration differ by a factor of 20. For Fig. 1 the stock solution was clarified by filtrating three times through one 5·0 μm pore size membrane filter. Correspondingly, stock solutions for Figs 2 and 3 were obtained after usage of 5·0/1·2 μm and 5·0/1·2/0·8/0·45 μm membranes three times each at the relevant pore size. It can easily be seen that the shape of the Zimm plots is strongly similar to those presented in Part I of this series. The solution behaviour of the measured data indicates clearly that with increasing concentration its apparent molecular weights increase or, in other words, an association occurs.

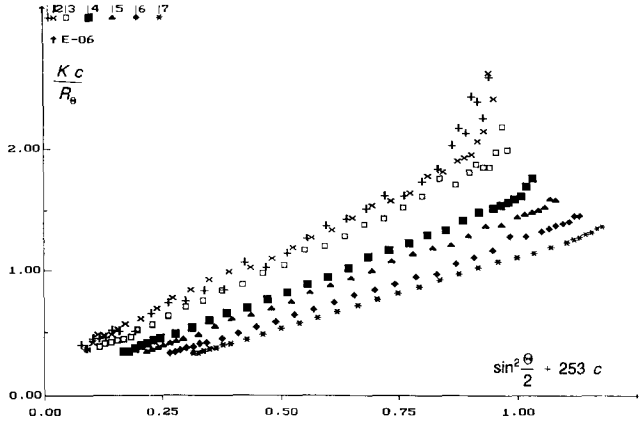

(a)

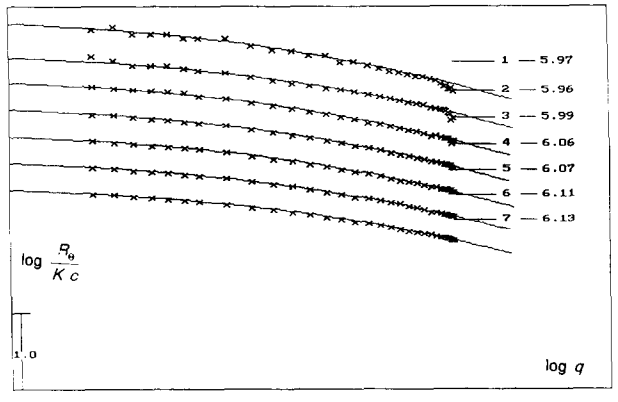

(b)

Fig. 3. (a) Zimm and (b) master plot obtained on a concentration series after filtration through a 0·45 μm pore size filter (see Table 1).

As usual the quality of the measured data depends on the absolute scattering level. That is why low concentrations after sharp filtration have a markedly higher experimental error (see, e.g. the upward curvature in the wide angle region). Nevertheless, all data allow an unambiguous interpretation by means of master curves in terms of one-component systems, in accordance with Part II (Fig. 2). Results of curve fitting are summarized in Table 1. They uniformly show no influence on the a_m value in the fifth column, whereas the average molecular weights M_W and hence the average densities ρ are growing with increasing polymer concentration. Evidently, the largest species of the population, which govern the angular dependence of the scattered light, do not suffer any change dependent on the concentration. The increase of the scattering level must be due to an association of relatively small individuals to species whose dimensions either remain small or do not exceed at least those of the large particles.

Comparable results were obtained when we *diluted* a pectin solution within the measuring cell (Fig. 4) although the dilution factor was only 2·5. This means a reversible association, whereas the gelation with sugar cannot simply be reversed. Association and gelation seem to have in common the fact that they are caused preferably by species from the medium molecular weight range, which carry short side chains (Berth & Dahme, 1991; Hwang & Kokini, 1991). Due to the lack of further information no quantitative approach can be attempted.

Zimm plots obtained on a dilution series of ultracentrifuged and subsequently membrane filtered solutions show a quite different shape (Fig. 5(a)–(c)). (Unfortunately, we could not prevent some distorting reflections within the wide angle region above 135°. They led to the strong downward curvature, which was neglected.) The filtrate of 0·45 μm gave rise to a slight downward curvature in the low angle domain and is, all in all, consistent with former findings in Part II.

Contrary to the previously applied Zimm analysis we have not shifted the curves along the x-axis. This was done in order to illustrate more clearly an effect which all the three last plots have in common to varying extents. It becomes obvious when these plots are compared with a 'normal' one in Fig. 6, as was obtained on dextran sulphate (see also Part I). Here, the individual curves at constant concentration are practically equidistant within the whole angular region with the highest concentration at a given angle on the top of the set and the lowest one on the bottom. This type of Zimm plot could be approximately achieved for the sharply filtered (0·45 μm) supernatant in Fig. 5(c). A comparable tendency is found in Fig. 5(a) and (b) only within the wide angle region. The smaller the angle the closer together the curves are. This means practically no concentration dependence of $k \cdot c/R_\theta$ at small angles, and hence B values close to zero. These relationships once again become more understandable on the basis of the two-component considerations introduced in Parts I and II. At low angles where $x_2 M_{W_2}$ governs the light scattering behaviour of the solution we measure the main properties of the particulate matter for which B values of zero are quite typical. In the wide angle region where traces of particulate matter no longer play a dominant role ($x_1 M_{W_1} \gg x_2 M_{W_2}$) the solution behaviour of the major molecularly dispersed component is seen. In this case we cannot find any evidence of association.

After all that has been pointed out, up to now it does not seem sensible to interpret the Zimm plots in Fig. 5(a) and (b) in classical terms. The alternative is to use the master plots shown in Fig. 7(a) and (b). They reflect clearly the bimodal distribution of the scattering species and do not indicate essential changes from one concentration to another within one series. For that reason we did not carry out a detailed analysis to give data comparable with Table 1.

Figure 5(c) is the only one out of the set which can

Table 1. Results of master curve interpretation for Figs 1–3 (concentration series—citrus pectin in phosphate buffer)

Fig.	Curve (symbol/no.)	Concentration ($g\,ml^{-1}$)	Model: spheres of homogeneous density				
			δ	a_m (nm)	M_W	$\rho(g/ml)$	$\langle s^2\rangle^{1/2}$ (nm)
1	+ 1	$4{\cdot}875\times10^{5}$	0·700	232·0	$1{\cdot}795\times10^{8}$	$5{\cdot}693\times10^{-3}$	612
1	× 2	$9{\cdot}870\times10^{5}$	0·700	217·3	$1{\cdot}890\times10^{8}$	$7{\cdot}301\times10^{-3}$	573
1	□ 3	$1{\cdot}974\times10^{4}$	0·700	219·0	$2{\cdot}249\times10^{8}$	$8{\cdot}497\times10^{-3}$	577
1	■ 4	$3{\cdot}948\times10^{4}$	0·700	212·6	$2{\cdot}382\times10^{8}$	$9{\cdot}824\times10^{-3}$	561
1	◇ 5	$5{\cdot}922\times10^{4}$	0·700	222·9	$2{\cdot}875\times10^{8}$	$1{\cdot}029\times10^{-2}$	588
1	◆ 6	$7{\cdot}896\times10^{4}$	0·700	219·7	$2{\cdot}872\times10^{8}$	$1{\cdot}073\times10^{-2}$	578
1	* 7	$9{\cdot}870\times10^{4}$	0·700	213·4	$2{\cdot}838\times10^{8}$	$1{\cdot}158\times10^{-2}$	563
2	+ 1	$4{\cdot}875\times10^{5}$	0·600	174·0	$6{\cdot}053\times10^{7}$	$4{\cdot}555\times10^{-3}$	332
2	× 2	$9{\cdot}870\times10^{5}$	0·600	149·2	$3{\cdot}994\times10^{7}$	$4{\cdot}173\times10^{-3}$	297
2	□ 3	$1{\cdot}974\times10^{4}$	0·600	155·9	$5{\cdot}077\times10^{7}$	$5{\cdot}305\times10^{-3}$	297
2	■ 4	$3{\cdot}948\times10^{4}$	0·600	154·8	$5{\cdot}529\times10^{7}$	$5{\cdot}905\times10^{-3}$	295
2	◇ 5	$5{\cdot}922\times10^{4}$	0·600	153·7	$5{\cdot}658\times10^{7}$	$6{\cdot}176\times10^{-3}$	293
2	◆ 6	$7{\cdot}896\times10^{4}$	0·600	152·6	$6{\cdot}182\times10^{7}$	$6{\cdot}897\times10^{-3}$	291
2	* 7	$9{\cdot}870\times10^{4}$	0·600	153·7	$6{\cdot}355\times10^{7}$	$6{\cdot}938\times10^{-3}$	293
3	+ 1	$4{\cdot}875\times10^{5}$	0·600	90·9	$3{\cdot}514\times10^{6}$	$1{\cdot}853\times10^{-3}$	173
3	× 2	$9{\cdot}870\times10^{5}$	0·600	85·5	$3{\cdot}027\times10^{6}$	$1{\cdot}922\times10^{-3}$	163
3	□ 3	$1{\cdot}974\times10^{4}$	0·600	88·6	$3{\cdot}437\times10^{6}$	$1{\cdot}956\times10^{-3}$	169
3	■ 4	$3{\cdot}948\times10^{4}$	0·600	87·0	$3{\cdot}915\times10^{6}$	$2{\cdot}354\times10^{-3}$	166
3	◇ 5	$5{\cdot}922\times10^{4}$	0·600	83·9	$3{\cdot}822\times10^{6}$	$2{\cdot}563\times10^{-3}$	160
3	◆ 6	$7{\cdot}896\times10^{4}$	0·600	82·1	$4{\cdot}022\times10^{6}$	$2{\cdot}880\times10^{-3}$	157
3	* 7	$9{\cdot}870\times10^{4}$	0·600	78·6	$4{\cdot}001\times10^{6}$	$3{\cdot}267\times10^{-3}$	150

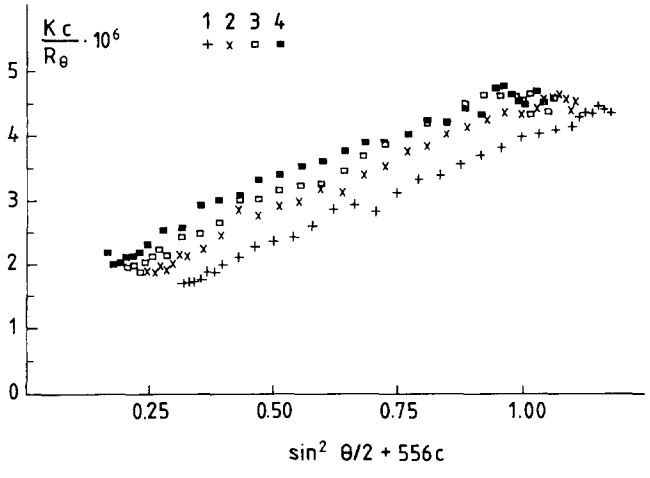

Fig. 4. Zimm plot obtained on a dilution series after filtering the stock solution and buffer through a 0·45 μm pore size filter.

be expected to give relatively reliable results when interpreted in terms of a Zimm plot. Figure 8 presents the (normal) concentration-shifted version of Fig. 5(c), where the arbitrary constant k has a negative sign. (Otherwise the curves overlap.) The molecular weight obtained ($M_W \sim 147\,000$) is somewhat higher than that followed from sedimentation analysis ($M_W = 90\,000 \pm 10\,000$; Harding *et al.*, 1991). The small B values which have been found ($B \sim 1{\cdot}0 \times 10^{-4}\,ml\,mol\,g^{-2}$) suggest residual particulate matter which is consistent with the downward curvature of the curves in Fig. 8. This is likely to be responsible for the difference between the light scattering and ultracentrifuge results.

The molecular weight of 147 000 is not so distant from the results published by Plashchina *et al.* (1985). When they studied a sample series of varying degree of esterification by light scattering after purification/clarification by means of ultracentrifugation and membrane filtration through 0·45 μm pore size filters they found molecular weights around 180 000, but definitely higher B values between $0{\cdot}9 \times 10^{-3}$ and $3{\cdot}0 \times 10^{-3}\,ml\,mol\,g^{-2}$. Like us they could not observe a tendency of association/aggregation under these conditions.

From that it appears that the ultracentrifuge has a serious effect, not only on the order of magnitude of molecular weights, but also on the solution behaviour. Species giving rise to the concentration-dependent and reversible association in Figs 1–4 could obviously be removed by centrifugation (see also Part II of this series). This means it is not the molecularly dispersed material which initiates association.

In contrast to our clarification studies we cannot yet generalize these findings. They may be relevant to observations made when we compared the parameters of gels prepared from centrifuged and non-centrifuged high-methoxyl pectins (Dahme, A. & Berth, G., unpublished). Fracture point and elastic shear modulus were quite different, and the effects varied strongly from one pectin to another. The pH value (Sawayama *et al.*, 1988) and the ionic strength might also play a role in association.

Maybe further studies in this field will be not only of

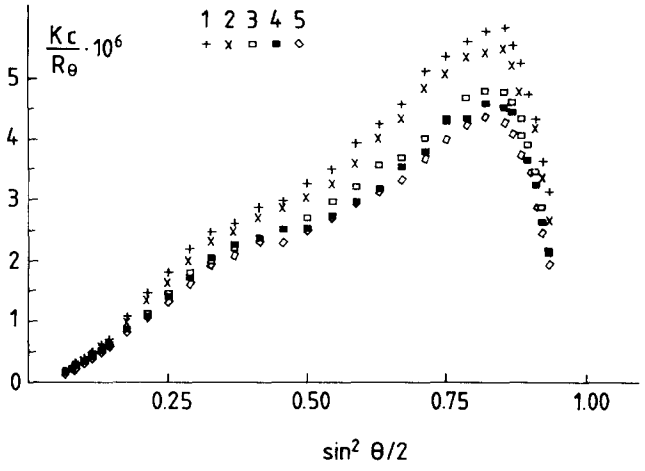

(a)

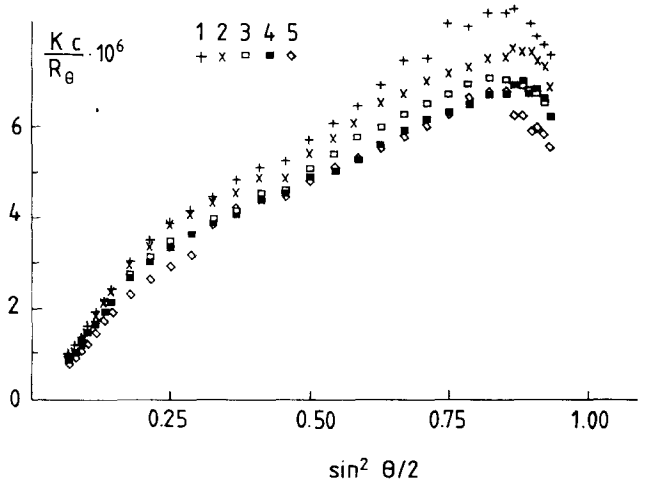

(b)

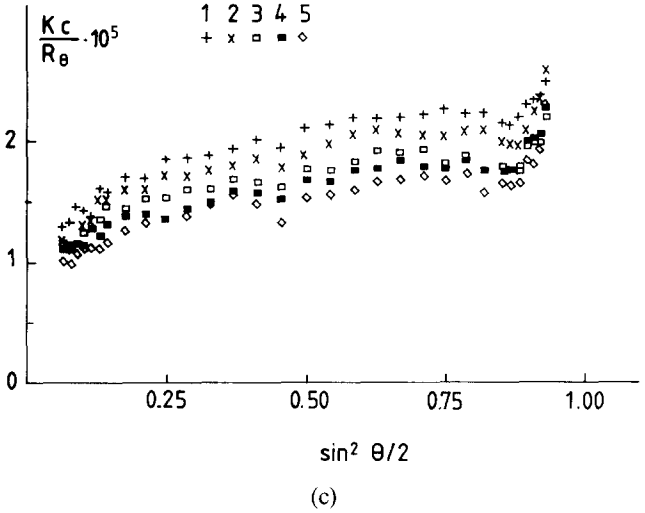

(c)

Fig. 5. Zimm plots obtained on a dilution series after filtrating the ultracentrifuged stock solution through a (a) 5·0, (b) 1·2, and (c) 0·45 μm pore size filter.

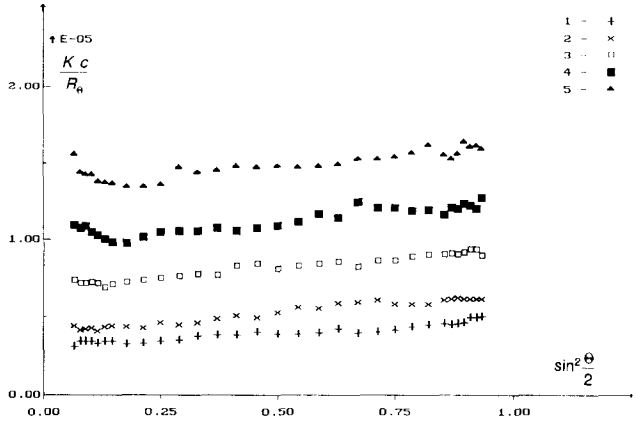

Fig. 6. Zimm plot for dextran sulphate in phosphate buffer (see Part I of this series).

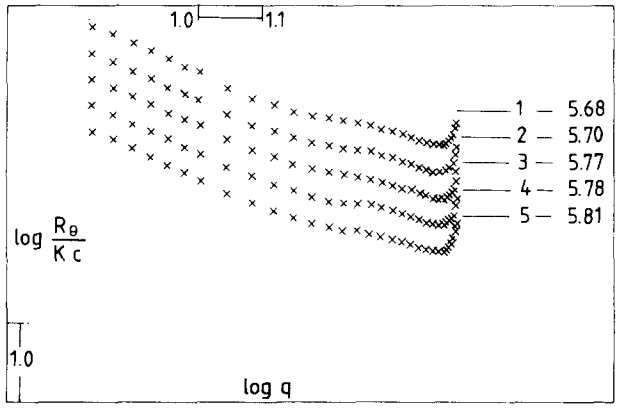

(a)

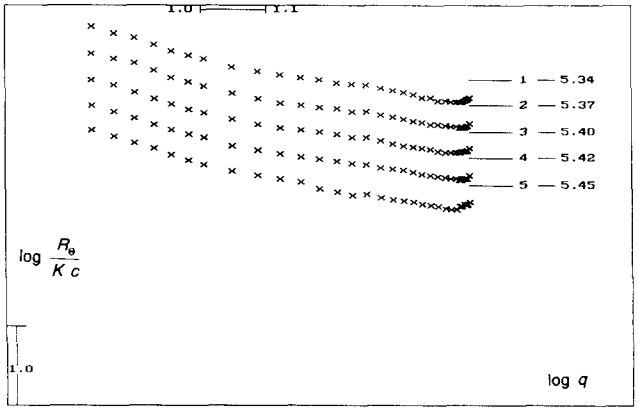

(b)

Fig. 7. Master plots corresponding to (a) Fig. 5(a) and (b) Fig. 5(b).

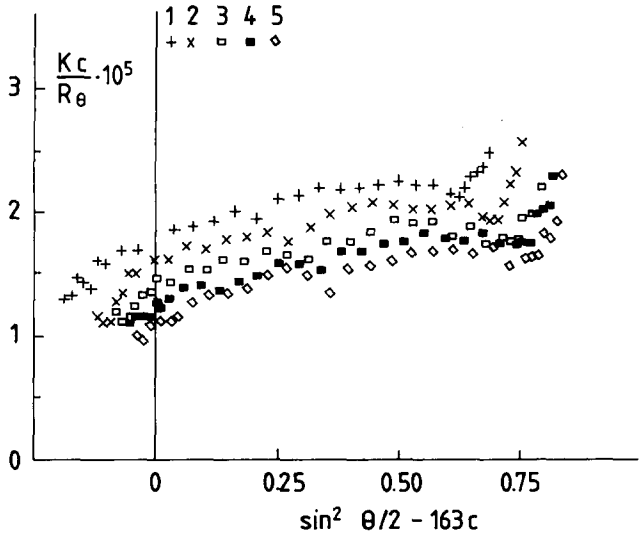

Fig. 8. Zimm plot with concentration shift (for details see Fig. 5(c)); $M_W = 147\,000$; $B = 1{\cdot}05 \times 10^{-4}$ ml mol g^{-2}.

an academic but also of an economic interest since the knowledge of the molecular weight alone is not the key for a better understanding of gelation (Berth, G. & Dahme, A., 1991).

ACKNOWLEDGEMENT

We thank Mrs Evelyn Lück in Potsdam-Rehbrücke for her careful laboratory assistance.

REFERENCES

Berth, G. & Dahme, A. (1991). *Food Hydrocoll.*, **5**, 101–4.
Berth, G., Dautzenberg, H. & Rother, G. (1994*a*). *Carbohydr. Polym.*, **25**, 177–85.
Berth, G., Dautzenberg, H. & Rother, G. (1994*b*). *Carbohydr. Polym.*, **25**, 187–95.
Dautzenberg, H. & Rother, G. (1988). *J. Polym. Sci., Part B, Polym. Phys.*, **26**, 353–66.
Dautzenberg, H. & Rother, G. (1992). *Makromol. Chem., Makromol. Symp.*, **61**, 94–113.
Harding, S.E., Berth, G., Ball, A., Mitchell, J.R. & de la Torre, G. (1991). *Carbohydr. Polym.*, **16**, 1–15.
Hwang, J. & Kokini, J.L. (1991). *J. Text. Stud.*, **22**, 123–67.
Plashchina, I.G., Semenova, M.G., Braudo, E.E. & Tolstogusov, V.B. (1985). *Carbohydr. Polym.*, **5**, 159–79.
Sawayama, S., Kawabata, A., Nakahara, H. & Kamata, T. (1988). *Food Hydrocoll.*, **2**, 31–7.
Smith, J.E. & Stainsby, G. (1977). *Br. Polym. J.*, **9**, 284.
Zimm, B.H. (1948). *J. Chem. Phys.*, **16**, 1099–116.